

Functional Classification of the Medial Ulnar Collateral Ligament

An In Vivo Kinematic Study With Computer-Aided Design

Erica Kholinne,^{*,†} MD, Rizki Fajar Zulkarnain,[†] MSc, Hyun-Joo Lee,[‡] MD, Arnold Adikrishna,[†] MSc, and In-Ho Jeon,^{†§} MD, PhD

Investigation performed at Asan Medical Center, University of Ulsan College of Medicine, Seoul, Republic of Korea

Background: It has been widely accepted that the anterior and posterior bundles of the medial ulnar collateral ligament (MUCL) tighten at extension and flexion, respectively. However, this belief is based on anatomic data acquired from cadaveric studies. The advancement of 3-dimensional (3D) model technology has made possible the simulation of dynamic movement that includes each ligament bundle fiber to analyze its functional properties. To date, no study has analyzed ligament kinematics at the level of the fibers while also focusing on their functional properties.

Purpose: To propose a new classification for functional properties of the MUCL based on its kinematic pattern.

Study Design: Descriptive laboratory study.

Methods: Five healthy elbow joints were scanned by use of computed tomography, and 3D models were rendered and translated into vertex points for further mathematical analysis. The humeral origin and ulnar insertion of the MUCL fiber groups were registered. Each vertex point on the origin side was randomly connected to the insertion side, with each pair of corresponding points defined as 1 ligament fiber. Lengths of all the fibers were measured at 1° increments of elbow range of motion (ROM). Ligament fibers were grouped according to their patterns. Mean coverage area for each group, expressed as the percentage of ligament fibers per group to the total number of fibers, was calculated.

Results: Four major bundle groups were found based on fiber length properties. Kinematic simulation showed that each group had a different kinematic function throughout elbow ROM. Mean coverage area of groups 1, 2, 3, and 4 was 8% ± 4%, 10% ± 5%, 42% ± 6%, and 40% ± 8%, respectively. Each group acted as a dominant stabilizer in certain arcs of motion. Reciprocal activity was observed between groups 1 and 3 along with groups 2 and 4 to produce synergistic properties of maintaining elbow stability.

Conclusion: Detailed analysis of fibers of the MUCL allows for further understanding of its kinematic function. This study provides MUCL group coverage area and kinematic function for each degree of motion arc, allowing selective reconstruction of the MUCL according to mechanism of injury.

Clinical Relevance: Understanding the dominant functional fibers of the MUCL will benefit surgeons attempting MUCL reconstruction and will enhance further anatomic study.

Keywords: elbow; imaging; medial ulnar collateral ligament; MUCL; functional classification; kinematic

The medial ulnar collateral ligament (MUCL) complex consists of 3 components: the anterior, posterior, and transverse bundles. It has been widely accepted that the anterior bundle is taut during elbow extension and the posterior bundle is taut during flexion. The transverse bundle joins the anterior and posterior bundles, but its function is not clearly defined. The anterior bundle of the MUCL is further divided into 2 functional components: anterior and

posterior bands that alternatively tighten and loosen throughout elbow range of motion.^{6,11,19} Some authors include a third central band^{12,15,16} and have categorized the anterior bundle of the MUCL into 3 types of bands: the anterior band is taut in full extension, the posterior band is taut between mid- and full flexion, and the central band is always taut throughout the full range of elbow motion. However, this system is based on anatomic data acquired from cadaveric studies rather than functional properties such as in vivo kinematic data. Moreover, it is practically impossible to measure every single fiber length in cadaveric studies due to the time needed and specimen's decomposition.

TABLE 1
Terms and Definitions

Term	Definition
Fiber-scale ligament partition	A concept of separating a ligament into fiber components to evaluate local behavior.
Growing region	A function mode to classify a pixel-based image segmentation method that involves the selection of initial seed points. Seed points will be recognized with a threshold created in advance by its similar threshold value.
Vertex	The endpoint where 2 lines will meet.
Cloud points	A set of data points consisting of coordinates in a 3-dimensional system.

To our knowledge, no study has evaluated the length properties of each MUCL fiber separately, which we refer to as *fiber-scale ligament partition* (see definitions in Table 1). By measuring the change in fiber length, we can determine which fiber plays a major role in supporting elbow stability at a certain range of motion. To achieve this, a detailed and accurate process that is less subject to human error is needed. This study used a reverse engineering method with medical image processing software to allow an anatomic segmentation from the original computed tomography (CT) scan image file. The method has previously been shown to provide anatomic registration to analyze MUCL fiber length in an accurate and noninvasive manner.^{13,14}

This study was designed to analyze the change in length of MUCL ligament fibers in the 3-dimensional (3D) setting of elbow dynamic movement simulation, from full extension to flexion, with 1° increments. We hypothesized that based on the grouping of fiber function, we could provide functional classification of the MUCL. The results of this study could be useful for surgeons when attempting MUCL reconstruction surgery and for further anatomic study.

METHODS

Image Acquisition and 3D Model Reconstruction

After institutional review board approval was granted, the right elbows of 5 volunteers (mean age, 32.4 years) with no history of upper extremity trauma or disorders were CT scanned at neutral rotation. The images were saved in DICOM (Digital Imaging and Communications in Medicine) file format. Serial CT images were arranged, and 3D models of the elbow were reconstructed by use of Mimics

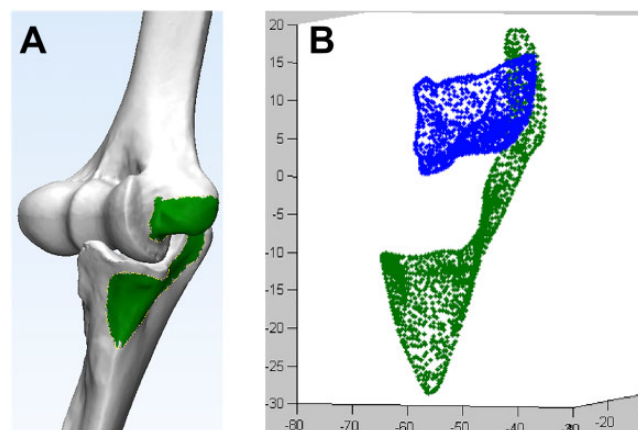


Figure 1. (A) Footprint registration for the humeral and ulnar sides of the medial ulnar collateral ligament using the freeform patch function. (B) Selected areas exported into a cloud of vertex points.

software (Mimics Research 17.0; Materialise). Single threshold-based methods were applied for bone segmentation. Growing region methods were used to separate humeral and ulnar bone segments. Using 3D Workspace (3-matic Research 9.0, Materialise), these reconstructed 3D models were converted into an STL file format to allow importation into other software.

Footprint Selection and Axis Determination

In a pilot study, a fresh cadaveric elbow was dissected to the bone, and the ligaments were retained. Several gross anatomic images were taken. The elbow underwent 3D CT for bone and ligament reconstruction. Based on the overlay images and several anatomic references from previous studies,^{3,6,9,10,12} the footprint of the MUCL on the humeral and ulnar sides was registered using the freeform patch function in 3-matic software (3-matic Research 9.0; Materialise). Selected areas were then exported into a cloud of 3D vertex points for mathematical analysis (Figure 1).

Geometric center points of the spherical capitellum and circular trochlear groove were determined by the centroid of a circle-fitted surface-tracing method from the cross-section of the distal humerus.⁷ A best-fit line connecting these center points in all cross-sections was defined as the rotational axis.²⁰ This axis was based on several studies that indicated the center of rotation of the elbow was located in the medial aspect of the trochlea in the distal humerus.^{4,5,8}

[§]Address correspondence to In-Ho Jeon, MD, PhD, Department of Orthopedic Surgery, Asan Medical Center, University of Ulsan College of Medicine, 88, Olympic-ro 43-gil, Songpa-Gu, Seoul 05505, Republic of Korea (email: jeonchoi@gmail.com).

^{*}Department of Orthopedic Surgery, St Carolus Hospital, Jakarta, Indonesia.

[†]Department of Orthopedic Surgery, Asan Medical Center, University of Ulsan College of Medicine, Seoul, Republic of Korea.

[‡]Department of Orthopedic Surgery, Kyungpook National University Hospital, Daegu, Republic of Korea.

One or more of the authors has declared the following potential conflict of interest or source of funding: This study was supported by the Global Frontier Program through the National Research Foundation of Korea (NRF) and funded by the Ministry of Science and ICT (NRF-2012M3A6A3056425).

Ethical approval for this study was obtained from Asan Medical Center (ethical review No. 2015-039).

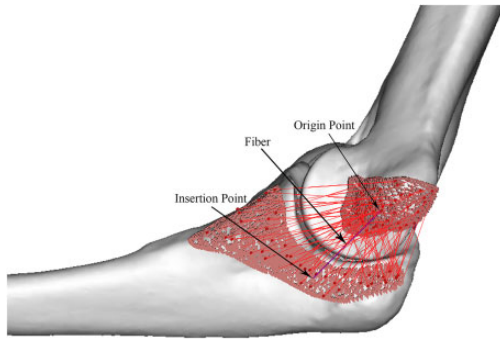


Figure 2. Ligament fiber definition. A fiber was represented as a line between 1 point at the humeral origin and 1 point at the ulnar insertion. The points at both sides were randomly connected to each other.

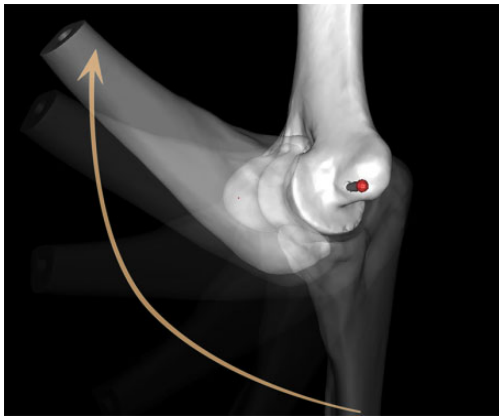


Figure 3. Simulated elbow movement with rotational axis as reference point from full extension (0°) to full flexion (135°) with neutral forearm rotation in 1° increments.

Ligament Length Kinematic Analysis and Fiber Groupings

The 3D cloud points and rotational axes were imported into MATLAB software (MATLAB and Statistics Toolbox Release 2013b; The MathWorks Inc). Cloud points consisted of more than 2000 vertex points for the humeral origin and ulnar insertion footprints. A ligament fiber was represented as a line connecting 1 vertex point at the humeral origin to 1 vertex point at the ulnar insertion, and the fiber length was defined as the distance between these 2 points (Figure 2). To render a complete human MUCL, each point at the origin side and each point at the insertion side were randomly connected to each other.

Elbow movement was simulated by moving the ulna relative to the humerus along the rotational axis from full extension (0°) to full flexion (135°) with neutral forearm rotation (Figure 3). Every ligament fiber length was recorded at 1° increments. The longest and shortest fibers recorded were defined as “tightening phase” and “loosening

phase” fibers, respectively. Fibers were grouped into maximum and minimum length patterns according to their similarity. The mean coverage area of each group was determined as the ratio of the number of fibers in each group to total number of fibers. Coverage was then outlined according to a clockface scheme, with medial epicondyle on face as 12 o'clock.

RESULTS

Categorizing the ligament fibers into similar patterns of maximum and minimum lengths revealed 4 major groups of fiber length changes throughout elbow range of motion (ROM) (Figure 4). The mean coverage area of each group (expressed as a percentage) is described in Table 2. Anatomic mapping of the fiber origin and insertion point of all groups is shown in Figure 5A.

In group 1, the ligament fiber lengths reached a maximum at 0° (full extension) and a minimum at 68° to 135° . The origin points were located at the superolateral humeral footprint (6-9 o'clock) (Figure 5B), and the mean coverage area of this group was $8\% \pm 4\%$. This ligament fiber group was the main elbow stabilizer at 0° , or full extension.

Group 2 fibers reached a maximum length at 1° to 67° (early flexion to midflexion) and a minimum length at 135° . The origin points were located at the superior humeral footprint (9-12 o'clock) (Figure 5C), and the mean coverage area of this group was $10\% \pm 5\%$. This group was the main elbow stabilizer at 1° to 67° of flexion.

Group 3 fibers reached a maximum length at 68° to 134° (midflexion to full flexion) and a minimum length at 0° . The origin points were located at the medial and posterosuperior humeral footprint (12-4 o'clock) (Figure 5D), and the mean coverage area of this group was $42\% \pm 6\%$. This group was the main elbow stabilizer at 68° to 134° and occupied the largest coverage area among all.

Group 4 fibers reached a maximum length at 135° (full flexion) and a minimum length at 0° to 67° . The origin points were located at the lateral inferior and posteroinferior humeral footprint (4-6 o'clock) (Figure 5E), and the mean coverage area of this group was $40\% \pm 8\%$. This group was the main elbow stabilizer at 135° , or full flexion.

DISCUSSION

Four different patterns of ligament fiber length were found throughout elbow ROM. The fibers were grouped according to these patterns (Figure 5A). Each group had an explicit location on the humeral origin footprint. From an anterior-posterior aspect, groups 1, 2, 3, and 4 were located at the lateral superior, medial superior, medial inferior, and lateral inferior side of the footprint, respectively. From the posterior aspect, group 3 predominated, followed by group 4. Our study showed a uniform and constant pattern for the humeral footprint and an obscure pattern for the ulnar insertion footprint. This could indicate that each fiber function during elbow flexion and extension is more dependent on its origin rather than its insertion.

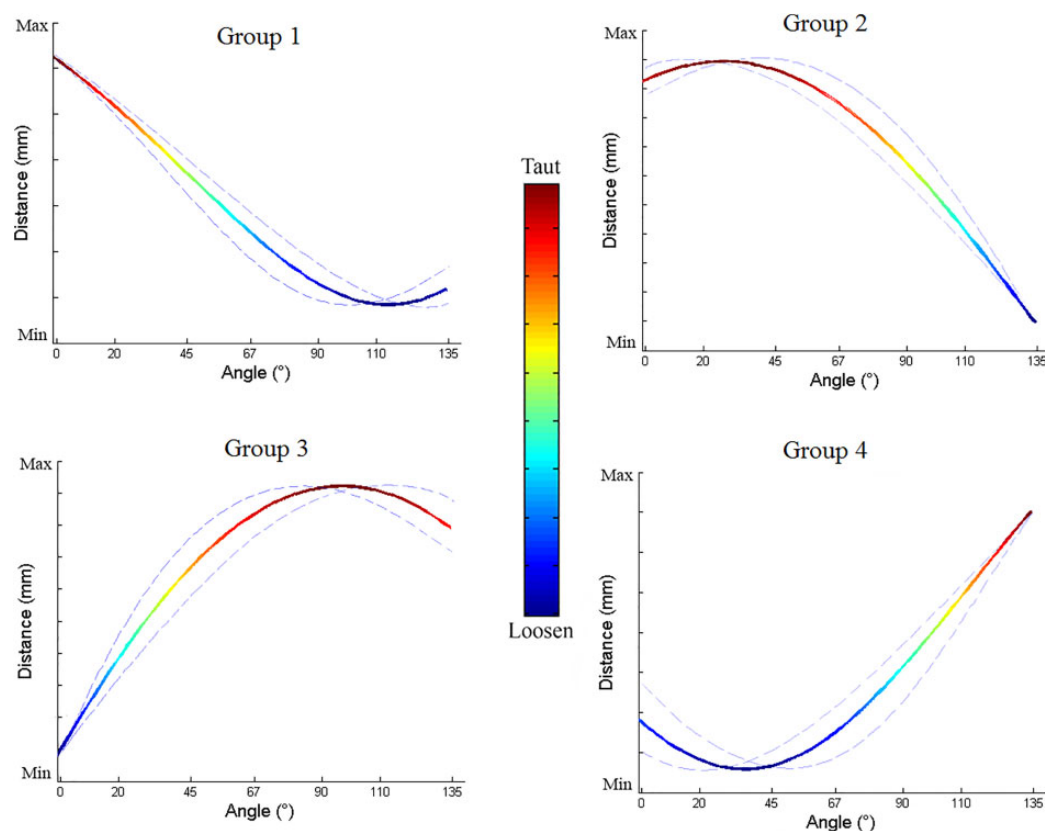


Figure 4. Four patterns of ligament fiber length changes during elbow motion. These patterns were established based on the similarity of the maximum and minimum lengths of each fiber.

TABLE 2
Mean Coverage Area of Each Fiber Group
for Each Patient Elbow^a

	Group 1 (0°)	Group 2 (1°-67°)	Group 3 (68°-134°)	Group 4 (135°)
Patient No.				
1	11	16	40	33
2	10	13	43	34
3	4	13	44	39
4	5	6	49	40
5	10	4	33	52
Mean ± SD	8 ± 4	10 ± 5	42 ± 6	40 ± 8

^aValues are expressed in percentages as the ratio of the number of fibers in each group to the total number of fibers. The angle at which each ligament fiber group represented the main elbow stabilizer is given in parentheses.

According to 2 studies,^{6,19} the anterior bundle of the MUCL is divided into 2 functional components: anterior and posterior bands. The authors stated that the anterior band is taut in extension and relaxed in flexion, while the posterior band behaves in a reciprocal fashion. Fuss¹² described 3 separate ligament groups based on functional distribution of attachment zones. Our study showed that, based on pattern similarity, ligament fiber

groups are overlaid rather than separated. We found 4 functional groups that interrelated gradually throughout the entire arc of motion. The most dominant group of fibers is located at 12 to 4 o'clock and serves as the main elbow stabilizer.

Our study also supports the abovementioned studies with more detailed findings. Our findings show that group 4 fibers are similar to the posterior band, while group 1 fibers are similar to the anterior band, which works reciprocally. Group 2 and 3 fibers are similar to those described as in the intermediate zone by Fuss.¹² These reciprocal features are also shown by functional pattern between groups 1 and 3 as well as groups 2 and 4. The patterns illustrate the synergistic properties of all fiber groups to maintain elbow stability throughout ROM. Santosgutierrez¹⁸ showed similar findings in that gradual reciprocal pressure between humeral and ulnar articular surfaces was produced by the ligaments.

Our study found no fibers that were isometric (SD = 0) in the MUCL, in contrast with previous reports.² Nevertheless, we found several fibers with minimum variation in length ($0 < SD < 0.2$ mm), which is practically isometric from a clinical point of view. The origins of these fibers were located near the rotational axis, which is the central vertex point of the intersection of all 4 pattern groups (Figure 5F). This position is similar to that of the guiding bundles described by Fuss,¹² which are located at intersection

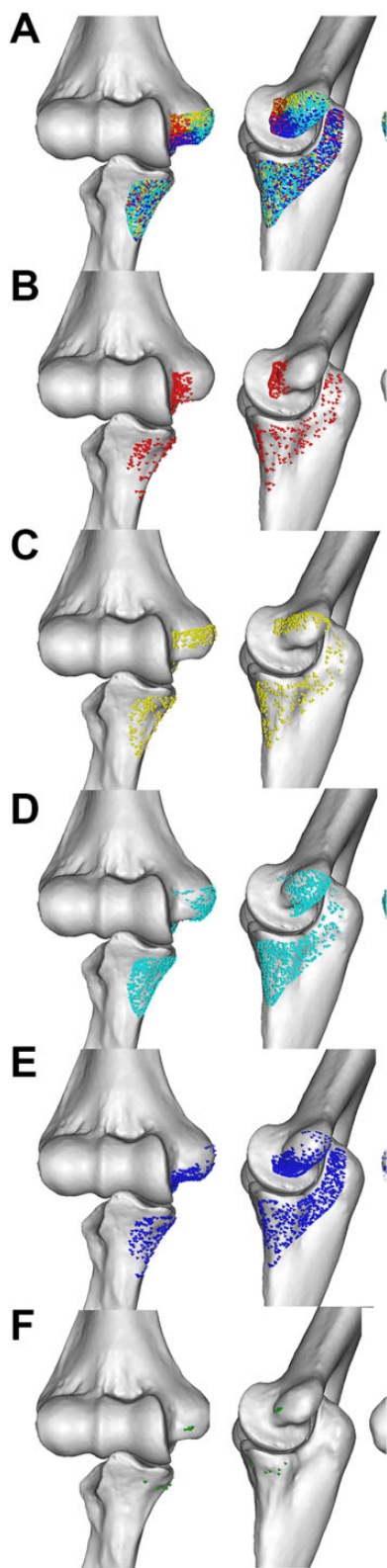


Figure 5. Anatomic mapping of fiber origin and insertion point (B) of group 1, (C) of group 2, (D) of group 3, (E) of group 4, and (F) near the isometric point location.

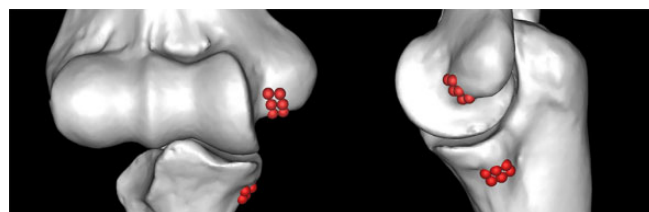


Figure 6. Illustration showing the origin and insertion sites of most isometric fibers.

zones. In contrast, these nearly isometric fibers had separate insertion points for ulnar footprints.

Each ligament fiber group had a separate vertex point, although the central vertex point for the ulnar site was not established. The overlaid figures of the ulnar footprints did not reveal a single central vertex, as they did for the humerus. From the obscure ulnar insertion pattern, most of the footprint occupied an area around the sublime tubercle (Figure 6). The locations were rather divergent compared with the humeral origin, which showed a central vertex point. This indicates that the isometric properties of ligament reconstruction would be independent of ulnar tunnel location, which validates the docking technique.¹⁷

Our results can help surgeons improve their MUCL reconstructions, especially when using docking and single-strand technique, by providing information on origin and insertion points preoperatively using CT.¹ In MUCL reconstruction surgery, an isometric graft is required¹; hence, the locations of the humeral and ulnar tunnels are important. Discrepancy in tunnel location may lead to anisometric properties of the grafts.

This study has several limitations. First, our study had a small number of subjects. Second, our fiber length model defined the distance between 2 points as a straight line, disregarding bony protrusions, which may reduce the similarities of the model to actual ligaments and may generate different calculated lengths. Third, we did not consider each fiber's torsion when active ROM was applied, and this may change the joint kinetics as well. Nevertheless, our study is the first to analyze the length properties of the MUCL in fiber resolution at 1° increments using thousands of reference points.

CONCLUSION

Plotting of fibers based on their function resulted in different mapping than currently reported for the morphology-based MUCL bundle complex. Detailed analysis of the fibers of the MUCL allows further understanding of its kinematic function. This study provides MUCL group coverage area and kinematic function for each degree of motion arc, allowing selective reconstruction of the MUCL according to the mechanism of injury. Thus, our findings will benefit surgeons when attempting MUCL reconstruction and will enhance further anatomic study.

REFERENCES

1. Ahmad CS, Lee TQ, ElAttrache NS. Biomechanical evaluation of a new ulnar collateral ligament reconstruction technique with interference screw fixation. *Am J Sports Med.* 2003;31:332-337.
2. Armstrong AD, Ferreira LM, Dunning CE, Johnson JA, King GJ. The medial collateral ligament of the elbow is not isometric: an in vitro biomechanical study. *Am J Sports Med.* 2004;32:85-90.
3. Axelrod TS. Exposures of the elbow. *Hand Clin.* 2014;30:415-425.
4. Bottlang M, Madey SM, Steyers CM, Marsh JL, Brown TD. Assessment of elbow joint kinematics in passive motion by electromagnetic motion tracking. *J Orthop Res.* 2000;18:195-202.
5. Bryce CD, Armstrong AD. Anatomy and biomechanics of the elbow. *Orthop Clin North Am.* 2008;39:141-154.
6. Callaway GH, Field LD, Deng XH, et al. Biomechanical evaluation of the medial collateral ligament of the elbow. *J Bone Joint Surg Am.* 1997;79:1223-1231.
7. Desai SJ, Deluce S, Johnson JA, et al. An anthropometric study of the distal humerus. *J Shoulder Elbow Surg.* 2014;23:463-469.
8. Duck TR, Dunning CE, King GJ, Johnson JA. Variability and repeatability of the flexion axis at the ulnohumeral joint. *J Orthop Res.* 2003;21:399-404.
9. Dugas JR, Ostrander RV, Cain EL, Kingsley D, Andrews JR. Anatomy of the anterior bundle of the ulnar collateral ligament. *J Shoulder Elbow Surg.* 2007;16:657-660.
10. Farrow LD, Mahoney AJ, Stefancin JJ, Taljanovic MS, Sheppard JE, Schickendantz MS. Quantitative analysis of the medial ulnar collateral ligament ulnar footprint and its relationship to the ulnar sublime tubercle. *Am J Sports Med.* 2011;39:1936-1941.
11. Floris S, Olsen BS, Dalstra M, Sojbjerg JO, Sneppen O. The medial collateral ligament of the elbow joint: anatomy and kinematics. *J Shoulder Elbow Surg.* 1998;7:345-351.
12. Fuss FK. The ulnar collateral ligament of the human elbow joint: anatomy, function and biomechanics. *J Anat.* 1991;175:203-212.
13. Goto A, Leng S, Sugamoto K, Cooney WP III, Kakar S, Zhao K. In vivo pilot study evaluating the thumb carpometacarpal joint during circumduction. *Clin Orthop Relat Res.* 2014;472:1106-1113.
14. Goto A, Moritomo H, Murase T, et al. In vivo elbow biomechanical analysis during flexion: three-dimensional motion analysis using magnetic resonance imaging. *J Shoulder Elbow Surg.* 2004;13:441-447.
15. Ochi N, Ogura T, Hashizume H, Shigeyama Y, Senda M, Inoue H. Anatomic relation between the medial collateral ligament of the elbow and the humero-ulnar joint axis. *J Shoulder Elbow Surg.* 1999;8:6-10.
16. Regan WD, Korinek SL, Morrey BF, An KN. Biomechanical study of ligaments around the elbow joint. *Clin Orthop Relat Res.* 1991;(271):170-179.
17. Rohrbough JT, Altchek DW, Hyman J, Williams RJ III, Botts JD. Medial collateral ligament reconstruction of the elbow using the docking technique. *Am J Sports Med.* 2002;30:541-548.
18. Santosgutierrez L. A contribution to the study of the limiting factors of elbow extension. *Acta Anat.* 1964;56:146-156.
19. Schwab GH, Bennett JB, Woods GW, Tullos HS. Biomechanics of elbow instability: the role of the medial collateral ligament. *Clin Orthop Relat Res.* 1980;(146):42-52.
20. Shiba R, Sorbie C, Siu DW, Bryant JT, Cooke TD, Wevers HW. Geometry of the humeroulnar joint. *J Orthop Res.* 1988;6:897-906.